Optimized angle scanning method for array sample detection in surface plasmon resonance biosensor

Pan Qi,[1,2] Ying Li,[3] and Jingang Zhong[1,3,*]

[1]Department of Optoelectronic Engineering, Jinan University, Guangzhou 510632, China

[2]Department of Electronics Engineering, Guangdong Communication Polytechnic, Guangzhou 510650, China

[3]Laboratory of Optoelectronic Information and Sensing Technologies of Guangdong Higher Education Institutes, Jinan University, Guangzhou 510632, China

*Corresponding author: tzjg@jnu.edu.cn

Received 19 August 2011; revised 25 October 2011; accepted 2 November 2011; posted 2 November 2011 (Doc. ID 153001); published 14 March 2012

An optimized angle scanning method is presented for array sample detection in a surface plasmon resonance biosensor. It provides a way to find the optimal rotation axis in the prism to resolve the drifting problem of the light incidence point on samples in the plane prism-coupling mode. The detection of array samples can be achieved by the translation of the prism along a particular direction. The validity of this method is theoretically analyzed and demonstrated by experiments. © 2012 Optical Society of America

OCIS codes: 240.6680, 120.0120, 280.1415.

1. Introduction

A surface plasmon resonance (SPR) biosensor is one of the most advanced label-free biosensors and has been widely applied in the studies of biomolecular interactions and the detection of chemical analytes [1]. Various SPR biosensors have been developed for different purposes, which can be classified as SPR sensors with prisms [2], gratings [3], and optical waveguides [4]. The most widespread applied SPR sensors are instruments with a prism coupler based on the Kretschmann configuration [5] for optical coupling of plasmons. In some applications, the multichannel detection of array samples is necessary. In order to increase the number of sensing channels, various platforms have been proposed. Most of them use imaging mode and are called SPR imaging [6–8]. A serious drawback of the SPR imaging instruments is that they measure reflectivity of light with a fixed angle. For accurate kinetic measurements of biomolecular interactions, only the shift of the near SPR dip is reliable, but an optimal fixed-angle position based on the inflection point of the SPR dip can only be found for one sample, not for all samples [1]. Of course, an SPR sensor has two working modes, one based on the angle scanning and one based on wavelength scanning [9]. Compared with the angle-scanning mode, the configuration of the wavelength-scanning mode is more complex and its measurement accuracy is lower. For the angle-scanning mode, a cylinder prism is usually used to ensure the incidence point of light on the sample will not drift when the incidence angle is changing as shown in Fig. 1(a), while the incidence point of light on the sample will drift in a plane prism-coupling mode as shown in Fig. 1(b). The sample is placed on the center of a semicircle, and the rotation center of the prism also should be at the center of the semicircle in the cylinder prism-coupling mode. Since each array sample cannot simultaneously be on the center of the semicircle, the cylinder prism-coupling mode cannot be applied to array samples. In order to realize angle scanning detection for the array samples, only the plane prism-coupling mode can be chosen. In a fan-shaped beam SPR instrument [1], the beam is focused on an infinitely narrow line on the sensor chip, and a charge-coupled device (CCD) is used to

1559-128X/12/091245-06$15.00/0

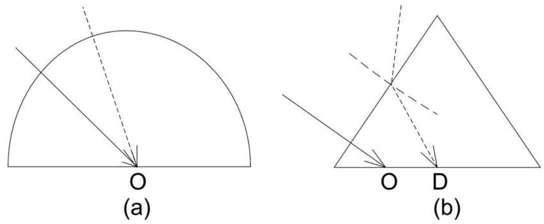

Fig. 1. Prism-coupling modes in SPR angle scanning. (a) Cylinder prism-coupling mode. (b) Plane prism-coupling mode.

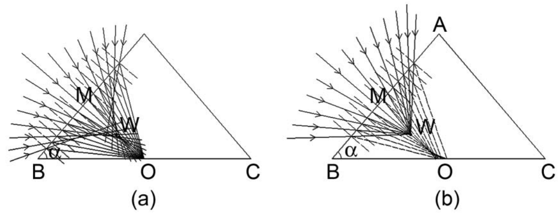

Fig. 3. (a) Geometric method to determine the optimal position of rotation axis. (b) Simulation of the positions that light rays incident on BC with W as rotation center.

determine the SPR dip position to avoid angle scanning. The drifting problem is automatically solved, but it is difficult to realize two-dimensional (2D) array samples detection in this way. To resolve the drifting problem of the light incidence point on samples in the plane prism-coupling mode, through careful analysis and calculation we find there is an optimal rotation axis in the prism. When the prism is rotating on this particular axis, the drift value of the point of incidence on the sample is minimal. The drift of the point of incidence will remain the minimum when the rotation axis moves along a particular direction. Thus, the detection of array samples can be achieved by the translation of the prism along a particular direction. In addition, for SPR biosensors, reflected light from the prism is measured. The reflected light can be easily collected by this method. In this paper, we will introduce an optimized angle-scanning method for array samples detection in SPR biosensors.

2. Optimized Angle-Scanning Method in Plane Prism-Coupling Mode

A. Determining the Optimal Rotation Axis

Without loss of generality, we choose an isosceles triangle prism as shown in Fig. 2 to demonstrate our method. The prism is a glass prism with refractive index n and is placed in air. ABC is the cross section of the isosceles prism; $AB = AC = a$; α is the base angle; Point O is on BC and point M is on AB. MO is perpendicular to AB. When the prism is rotating, the angle of incidence of a fixed light beam that is incident on the prism is also changing. The rotation axis L goes vertically through the cross section ABC of the prism at point W. We call point W the rotation

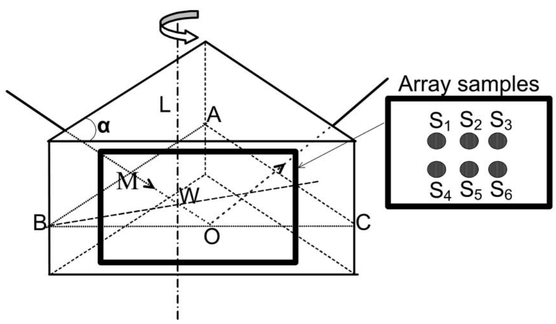

Fig. 2. Schematic of prism rotation and array samples.

center. S_1–S_6 are array samples. One of the samples is placed on the point O.

First, the geometric method is used to determine the optimal position of the rotation axis.

Figure 3(a) shows that when O is presumed to be a point light source, its light rays can enter the air medium through glass medium after refraction. On the basis of the reversibility principle of light, the refractive rays will converge at the point O if the refractive rays propagate back. We can draw the reverse extension lines of the refractive rays as the dotted lines in Fig. 3(a). If all the reverse extension lines intersect at one point, then we can set this point as the rotation center W. From Fig. 3(a), we find that the reverse extension lines have not intersected at one point. However, there is a relatively dense area of the intersect points. So, if we set the point W in this area, the drift value of incidence point of the light on the sample may be the minimum when the prism is rotating. Considering the symmetry, the point W should be set on normal line of AB. When the prism is rotating with the rotation center set as point W, and the light rays are incident into the prism at different angles, the positions that light rays are incident on BC are shown in Fig. 3(b). We find the incidence points on BC are basically around the point O. The different position of point W on the normal line OM will result in different situation of incidence point on BC.

Subsequently, a theoretical analysis is carried out in order to obtain the optimal position of point W on OM.

If the rotation center is set at point W, the initial incidence light ray I at point M is perpendicular to AB and will project onto the point O as shown in Fig. 4. When the prism rotates clockwise an angle θ, the incidence light ray is incident onto the prism with the incidence angle θ as the incidence light ray II shown in Fig. 4 and then refracted onto the point D. The incidence angle of light ray II on BC is ϕ. Point D is the deviation from point O with the deviation value OD. Point G is the middle of the height of the base side. We can calculate the deviation values with different positions of the point W on MO. When the deviation value OD is close to zero, we think the rotation center W is at an optimal position.

When the light ray is incident onto the prism with the incidence angle θ, OD can be calculated through the refraction law of light and geometric parameter of prism as

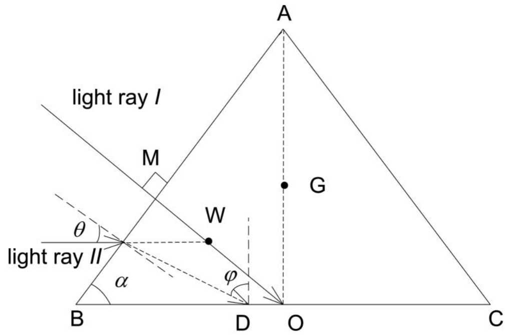

Fig. 4. Schematic of drift value when the prism rotated clockwise an angle θ with W as rotation center.

$$OD = a \cos\alpha - \cos\alpha(a\cos^2\alpha - MW\tan\theta) - \sin\alpha(a\cos^2\alpha - MW\tan\theta)\tan\phi, \quad (1)$$

and

$$\sin\theta = n\sin(\phi - \alpha). \quad (2)$$

When W is the optimal rotation center, the incidence point at the baseline staying the same ($OD = 0$), from Eq. (1), we have

$$MW = \frac{a\cos\alpha(\cos^2\alpha + \sin\alpha\cos\alpha\tan\phi - 1)}{\tan\{\arcsin[n\sin(\phi-\alpha)]\}(\cos\alpha + \sin\alpha\tan\phi)}, \quad (3)$$

and $MO = a\cos\alpha\sin\alpha$, so

$$\frac{MW}{MO} = \frac{\cos^2\alpha + \sin\alpha\cos\alpha\tan\phi - 1}{\sin\alpha\tan\{\arcsin[n\sin(\phi-\alpha)]\}(\cos\alpha + \sin\alpha\tan\phi)}. \quad (4)$$

The position of point W on OM can be determined by Eq. (3) or Eq. (4). Obviously, Eq. (3) and Eq. (4) are related to the incident angle ϕ; therefore there is not a common position of point W for all incident angles, and that is why the reverse extension lines have not intersected at one point as shown in Fig. 3(a). In SPR, we can estimate the value of resonance angle φ_0 if the approximate value of the refractive index of the sample is known beforehand. Setting $\phi = \varphi_0$, Eq. (3) and Eq. (4) can be presented as follows:

$$MW|_{\text{optimal}} = \frac{a\cos\alpha(\cos^2\alpha + \sin\alpha\cos\alpha\tan\varphi_0 - 1)}{\tan\{\arcsin[n\sin(\varphi_0-\alpha)]\}(\cos\alpha + \sin\alpha\tan\varphi_0)}, \quad (5)$$

$$\frac{MW}{MO}\Big|_{\text{optimal}} = \frac{\cos^2\alpha + \sin\alpha\cos\alpha\tan\varphi_0 - 1}{\sin\alpha\tan\{\arcsin[n\sin(\varphi_0-\alpha)]\}(\cos\alpha + \sin\alpha\tan\varphi_0)}. \quad (6)$$

The position of point W determined by Eq. (5) or Eq. (6) can ensure that the value OD is close to zero when the incident angle ϕ is close to the SPR resonance angle. So we take the rotation axis that is obtained by Eq. (5) or Eq. (6) as the optimal position.

A computer simulation can perform the drift situation when the rotation center is at the optimal position and describe the comparison of the drifting situation when the rotation center is at other positions, including at the center of the base side (O), the apex (A), and the middle of the height of base side (G) (see Fig. 4). The corresponding drifting values are presented as OD_{optimal}, OD_O, OD_A, and OD_G, respectively.

A right angle isosceles prism, which is the same as the one used in the experiment, is employed for analysis. The parameters of the prism are as follows: $n = 1.5163$ (glass K9), the length of waist and its thickness both are 3.25 cm, $\alpha = 45$ deg. The refractive index of the sample is close to that of distilled water, and the SPR resonance angle of distilled water is near 1.27 rad. Therefore, we take $\varphi_0 = 1.27$ rad in Eqs. (5) and (6), and we can get: $MW|_{\text{optimal}} \approx 0.956$ cm, $\frac{MW}{MO}|_{\text{optimal}} \approx 0.525$. Then, from Eqs. (1) and (2), we can have:

$$OD_{\text{optimal}} = \frac{3.25\sqrt{2}}{2} - \frac{3.25\sqrt{2}}{2}\left(\frac{1}{2} - \frac{0.525}{2}\tan\theta\right) \times \left\{1 + \tan\left[\frac{\pi}{4} + \arcsin\left(\frac{\sin\theta}{1.5163}\right)\right]\right\}. \quad (7)$$

And OD_O, OD_A, and OD_G can be calculated through the refraction law of light and geometric parameter of prism as follows:

$$OD_O = \frac{3.25\sqrt{2}}{2} - \frac{3.25\sqrt{2}}{4}(1 - \tan\theta) \times \left\{1 + \tan\left[\frac{\pi}{4} + \arcsin\left(\frac{\sin\theta}{1.5163}\right)\right]\right\}, \quad (8)$$

$$OD_A = \frac{3.25\sqrt{2}}{2} - \frac{3.25\sqrt{2}}{2}\left(1 - \frac{1}{2\cos\theta}\right) \times \left\{1 + \tan\left[\frac{\pi}{4} + \arcsin\left(\frac{\sin\theta}{1.5163}\right)\right]\right\}, \quad (9)$$

$$OD_G = \frac{3.25\sqrt{2}}{2} - \frac{3.25\sqrt{2}}{8}\left(3 - \tan\theta - \frac{1}{\cos\theta}\right) \times \left\{1 + \tan\left[\frac{\pi}{4} + \arcsin\left(\frac{\sin\theta}{1.5163}\right)\right]\right\}. \quad (10)$$

Finally, according to Eqs. (7)–(10), the simulation results of the above situations are determined as shown in Fig. 5.

Figure 5 clearly shows that when the rotation center is set at the optimal position with $\frac{MW}{MO}|_{\text{optimal}} = 0.525$, the drifting value OD is almost zero near the SPR resonance angle $\varphi_0 = 1.27$ rad (θ is near 0.792 rad). We can easily find that when the rotation center is set at other positions, the value of OD is significantly larger than that obtained from the optimal position near the SPR resonance angle.

B. Optimal Translation Direction of Prism for Detecting Array Samples

Detecting array samples can be achieved by moving the prism while the light source is fixed. After the optimal rotation axis is obtained by the above method for one sample spot, according to the geometric relationship, so long as the light source is fixed, we can ensure the rotation axis is always in the optimal position for other sample spots when the prism moves along a particular direction. We call the particular direction the optimal translation direction of the prism. The X direction shown in Fig. 6 is the particular direction that is throughout the point B, and the angle β can be calculated by the equation as follows:

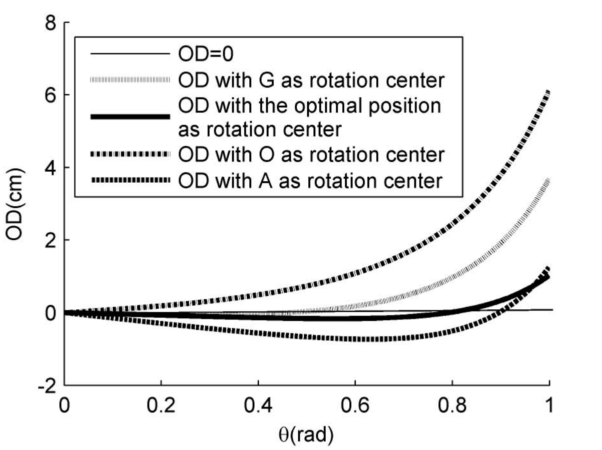

Fig. 5. Simulation of drifting values of the light incidence point with the optimal position, point G, point O, and point A as the rotation center.

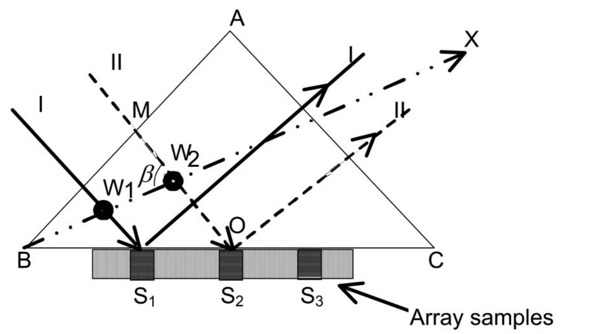

Fig. 6. Optimal translation direction of prism for array samples detection.

$$\frac{1}{\tan\beta} = \tan\alpha \frac{MW}{MO}|_{\text{optimal}}, \quad (11)$$

where $\frac{MW}{MO}|_{\text{optimal}}$ is given by Eq. (6). Obviously, when the prism moves along the particular translation direction, the rotation axis is always in the optimal position for each sample spot on the same row as S_1, S_2, and S_3, shown in Fig. 2. As for the detection of sample spots on a different row, they can be achieved by moving the prism along the direction perpendicular to cross section ABC of the prism. In Fig. 6, the solid line I and dashed line II is the incidence light ray for the sample spots S_1 and S_2 before and after the prism moves in X direction, with the optimal rotation centers W_1 and W_2, respectively.

3. Experiment

In order to verify our method, we constructed the measurement system shown in Fig. 7. A He-Ne laser with 250 mm cavity length is used for the light source. The double-prism is fixed on a rotation stage driven by a stepping motor. The parameters of the single prism are as follows: $n = 1.5163$ (glass K9), the length of waist and its thickness both are 3.25 cm, $\alpha = 45$ deg. The rotation angle of each step is set at 0.1 deg. A CCD camera fixed on the rotation stage is used to record the drifting situation of the detection light point at the gold film when the prism is rotating. A photoelectricity detector (PD) is used to measure the reflected light from the prism.

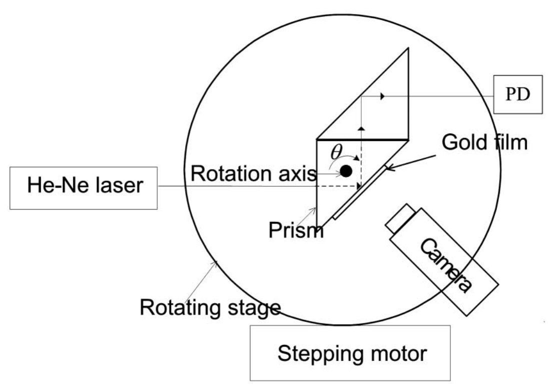

Fig. 7. Schematic of the measurement system.

Fig. 8 demonstrates the drifting situations of the light incidence point when the rotating stage rotates from 0 to 0.8 rad. Media 1 vividly reveals the drifting path of the light incidence point when the rotation center is set at point G and is recorded by the CCD. In Media 1, we can see clearly that the light incidence point at the gold film drifts in the positive direction (right is positive direction, left is negative direction) as θ increases, and the drifting value increases rapidly near 0.8 rad.

Media 2 shows when the rotation center is at point O, the drifting path of the light incidence point as θ rotates from 0 to 0.8 rad. The light incidence point at the gold film drifts in the positive direction as θ increases. The drifting value increases rapidly near 0.6 rad, and the light incidence point deviates from the gold film in the prism base side when it rotates 0.8 rad.

When the rotation center is set at point A, the drifting path of the light incidence point as θ rotates from 0 to 0.8 rad is vividly displayed in Media 3. From Media 3, we can clearly see that the light incidence point at the gold film drifts in the negative direction as θ increases. The maximum drifting value is near 0.7 rad, and the drifting value decreases slightly at 0.8 rad.

The drifting path of incidence point as θ rotates from 0 to 0.8 rad with the rotation center set at the optimal position can be clearly seen in Media 4. The light incidence point at the gold film slightly drifts in the negative direction as θ increases. The maximum drifting value is near 0.6 rad, and the drifting value decreases significantly in the range of 0.6 ~ 0.8 rad. What is more, the drifting value is close to zero when θ is near 0.8 rad.

In order to measure the actual drifting value OD of the light incidence point, we take pictures of the laser spot in the gold film when θ rotates at a certain angle,

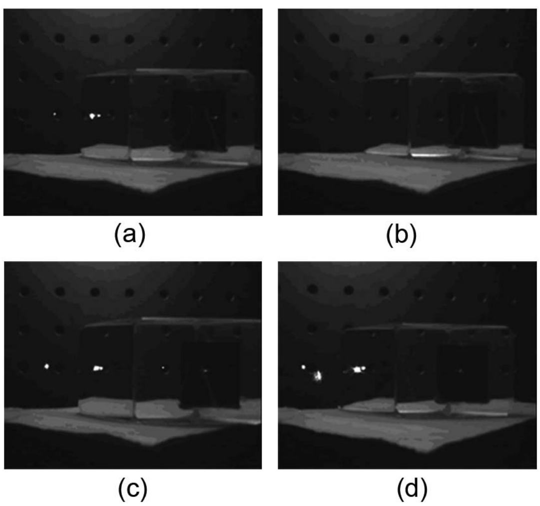

Fig. 8. Video of incidence point drifting situation when θ is in the range of $0 \sim 0.8$ rad for different rotation axes. (a) Point G is the rotation center (Media 1). (b) Point O is the rotation center (Media 2). (c) Point A is the rotation center (Media 3). (d) The optimal rotation center (Media 4).

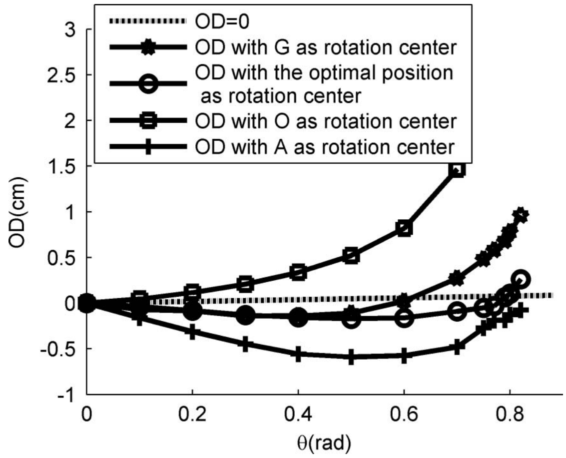

Fig. 9. Measure of drifting values with the optimal position, point G, point O, and point A as the rotation center.

with the optimal position of point G, point O, and point A as the rotation center, respectively. Then we get the coordinate (horizontal axis) of the geometric center of the laser spot (when $\theta = 0$ rad) by using the method of image processing, which is set as reference. After it rotates to a certain angle, the coordinate of the laser spot is changed. The drifting value OD can be calculated by finding the change value of the coordinates.

With the method above, the value of OD is calculated when θ is 0, 0.1, 0.2, 0.3, 0.4, 0.5, 0.6, 0.7, 0.75, 0.77, 0.79, 0.8, and 0.82 rad, as point G, point O, point A, and the optimal position is used as rotation center. The results are shown in Fig. 9. When the rotation center is set at point O, and $\theta \geq 0.75$ rad, the light incidence point deviates from the gold film, as its drifting value is huge.

The above results of our experiment fit with the results of the simulation. In the angle detection near the sample SPR resonance angle, we need to ensure the drifting value of the light incidence point to be minimized in the process of SPR biochemical analysis. From the results of the simulation (Fig. 5) and experiment (Fig. 8 and Fig. 9), it is obvious that the drifting value of the light incidence point is minimal when the rotation center is set at the optimal position obtained through above calculation.

To illustrate the advantage of using this improved angle-scanning method, a SPR sensing experiment is performed. Water is used as the sample. The sample cell is fixed on the gold film by an O-ring (see Fig. 10). The SPR angle is detected when θ rotates from 0.72 to 0.85 rad, and the rotation center is set at

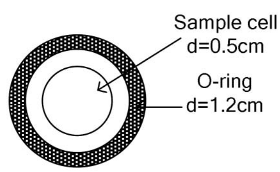

Fig. 10. Schematic of the sample cell.

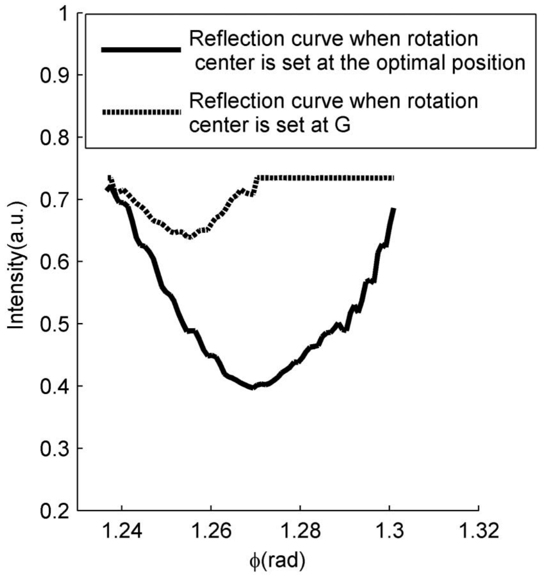

Fig. 11. Reflection curve of water when the rotation center is set at the optimal position and point G.

the optimal position and point G (see Fig. 4), respectively. The result is shown in Fig. 11.

The incidence light will not drift off the sample in the scan process when the optimal position is used as rotation center. We can get the whole curve of the SPR dip. The SPR angle of water can be detected accurately. As point G is used as the rotation center, the incidence light will drift off the sample when $\theta >$ 0.78 rad (corresponding $\phi > 1.267$ rad). We can only get part of the SPR dip curve. That means it needs a larger sample to complete the SPR detection if point G is used as the rotation center. Figure 11 clearly shows the advantage of using this improved angle-scanning method.

4. Conclusion

In this paper, an optimized angle-scanning detection method based on resonance angle detection is presented, which is applied to array samples detection in an SPR biosensor. We resolve the problem of the light incidence point tending to drift from samples by carefully designing the rotation axis position in the angle-scanning and the translation direction of the prism. This has significant importance for increasing the sample density of array samples and realizing a high precision and high throughput detection. In addition, the reflected light can be easily collected by this method.

This work was supported by National Natural Science Foundation of China (NSFC) under the Grant No. 61077003, Guangdong Natural Science Foundation under the Grant No. 8451063201000076, and breakthroughs in key areas of Guangdong and Hong Kong tender No. 2005A20501001.

References

1. R. B. M. Schasfoort and A. J. Tudos, eds., *Handbook of Surface Plasmon Resonance* (Royal Society of Chemistry, 2008).
2. B. Liedberg, C. Nylander, and I. Lundstrom, "Surface plasmon resonance for gas detection and biosensing," Sens. Actuators **4**, 299–304 (1983).
3. D. C. Cullen, R. G. Brown, and C. R. Lowe, "Detection of immuno-complex formation via surface plasmon resonance on gold-coated diffraction gratings," Biosensors **3**, 211–225 (1987/88).
4. R. D. Harris and J. S. Wilkinson, "Waveguide surface plasmon resonance sensors," Sens. Actuators B **29**, 261–267 (1995).
5. E. Kretschmann and H. Raether, "Radiative decay of non radiative surface plasmons excited by light," Z. Naturforsch. A **23**, 2135–2136 (1968).
6. B. Rothenhäusler and W. Knoll, "Surface-plasmon microscopy," Nature **332**, 615–617 (1988).
7. L. A. Lyon, W. D. Holliway, and M. J. Natan, "An improved surface plasmon resonance imaging apparatus," Rev. Sci. Instrum. **70**, 2076–2081 (1999).
8. A. G. Notcovich, V. Zhuk, and S. G. Lipson, "Surface plasmon resonance phase imaging," Appl. Phys. Lett. **76**, 1665–1667 (2000).
9. K. Johansen, H. Arwin, I. Lundström, and B. Liedberg, "Imaging surface plasmon resonance sensor based on multiple wavelengths: sensitivity considerations," Rev. Sci. Instrum. **71**, 3530–3538 (2000).